Theory of Miniaturized Shorting-Post Microstrip Antennas

Rebekka Porath

***Abstract*—An analytical theory for the eigenfrequencies and eigenmodes of shorting-post microstrip antennas (MPA's) is presented. These antennas are seen as promising candidates for miniaturized mobile telecommunication handsets. In particular, it is shown that the zero mode of the unloaded MPA plays a central role for reducing the lowest operation frequency of the loaded MPA. The theory allows a complete calculation of all relevant antenna parameters and can easily be extended to the case of multiple shorting posts. Applications to the examples of rectangular and circular shorting post MPA's are illustrated.**

***Index Terms*—Microstrip antennas.**

I. Introduction

DUE to the intrinsic low profile of microstrip antennas (MPA's), they are regarded as one of the promising candidates for advanced integrated antennas in strongly miniaturization-driven application fields such as mobile telecom. One approach to further reduce the lateral dimensions of MPA's consists of loading the antenna with one or several shorting posts, i.e., metallic vias connecting the patch to the ground plane. This technique as a measure to reduce the resonance frequency has first been proposed by Waterhouse [3] and has, in the meantime, been demonstrated on a variety of different patch shapes [4]. It has been shown that the resonance frequency depends critically on the position and the dimensions of the shorting post. These observations have largely been made on a phenomenological basis, i.e., on experimental or simulation results.

Earlier approaches to theoretically analyze the effect of loading-patch antennas with shorting posts have employed a variety of methods ranging from transmission-line models [5] to Green's function approaches based on the cavity model [6]. These works, however, have concluded that a shorting post MPA will display resonance frequencies above the lowest operation frequency of the unloaded patch antenna. Basically, the shorting post is modeled as an inductance parallel to a resonant (R)LC-circuit describing a reference resonant mode of the unloaded patch.

This paper gives a fully analytical theory for calculating the full spectrum of resonance frequencies of a shorting post MPA. It is shown that the zero mode of the unloaded MPA is the key for understanding and proving the existence of a resonance mode below the lowest operation frequency of the unloaded patch. In an equivalent circuit picture, this new resonance mode can be viewed as resulting from an inductance (due to the shorting post) in series with the static capacitance of the patch configuration.

Manuscript received July 21, 1998; revised October 14, 1999.

The author is with the Philips Research Laboratories, Aachen, 52066 Germany.

Publisher Item Identifier S 0018-926X(00)01276-X.

The presentation is subdivided into two sections. The first section describes the basic theory for calculating critical frequencies of an MPA embodying one shorting post. Considering the case with external feed, it is shown that these frequencies are equivalent to the poles of the input impedance of the driven lossless antenna and, therefore, to its resonant frequencies. Furthermore, it is indicated how the theory can be extended to the case of multiple shorting posts.

The second section illustrates the application of the theory with the examples of a rectangular and a circular MPA. Explicit expressions for the associated resonant cavity field distributions are included. These can be employed to calculate all radiation properties such as radiation patterns, quality factors, and efficiency.

II. Theory

Consider an arbitrarily shaped MPA dimensioned such as to satisfy the assumptions of the standard cavity model. For harmonically time dependent fields, the wave equation in the cavity region can be written as

$$(-\Delta - k^2)E_z(x,y) = i\omega\mu_0 j_z(x,y) \tag{1}$$

where $k := \omega\sqrt{\mu_0\varepsilon}$ (the relative permeability of the substrate being assumed equal to one) with electric- (top and bottom surface) and magnetic-wall (side surfaces) boundary conditions on the cavity surface. These boundary conditions uniquely determine the solution of (1) if k^2 does not coincide with an eigenvalue of the Laplace operator $-\Delta$. This unique solution can be determined in terms of the Green's function $G(xy, x'y')$ of the problem

$$E(x,y) = i\omega\mu_0 \int dx' \int dy'\, G(xy,x'y')(j(x',y'). \tag{2}$$

A shorting post at (x_0, y_0) requires vanishing of the field at this position and hence vanishing of the diagonal element $G(x_0y_0, x_0y_0)$ of Green's function. The diagonal elements of Green's functions in two dimensions are logarithmically singular. A regularization procedure relying on very small but nonvanishing shorting post diameter is, therefore, assumed. In terms of the eigenfunctions, ψ_{nm} and eigenvalues $\varepsilon_{nm} = k_{nm}^2 - k^2$ of the operator $(-\Delta - k^2)$, $G(xy, x'y')$ can be written as

$$G(xy,x'y') = \sum_{nm} \frac{\psi_{nm}(xy)\psi_{nm}(x'y')}{k_{nm}^2 - k^2} \tag{3}$$

and the requirement of vanishing diagonal element $G(x_0y_0, x_0y_0)$ can be understood as an equation for the determination of k^2

$$\frac{|\psi_{00}(x_0,y_0)|^2}{-k^2} + \sum_{(n,m)\neq(0,0)} \frac{|\psi_{nm}(x_0,y_0)|^2}{k_{nm}^2 - k^2} = 0. \tag{4}$$

The zero mode has been explicitly separated. The existence of this zero mode is generally sustained by the von Neumann boundary conditions. Equation (4) allows us to infer the existence of a solution $k_{(0)}^2$ with

$$0 \le k_{(0)}^2 \le k_{10}^2$$

since the sum tends to $\mp\infty$ at the lower/upper boarder of this interval (k_{10} is supposed to be the smallest nonzero eigenvalue). This leads to the important conclusion that there is a frequency $\omega_{(0)} = ck_{(0)}$ below the lowest eigenvalue k_{10}^2 of the Laplace operator: the insertion of the shorting post will allow for a smaller antenna at a given operation frequency.

To get the next solution $k_{(1)}$, rewrite (4) as

$$\frac{|\psi_{00}(x_0,y_0)|^2}{k^2} + \frac{|\psi_{10}(x_0,y_0)|^2}{-k_{10}+k^2} = \sum_{(n,m)\neq(0,0),(1,0)} \frac{|\psi_{nm}(x_0,y_0)|^2}{k_{nm}^2-k^2} = 0. \quad (5)$$

Both sides of the equation are positive in the interval $k_{10}^2 \le k^2 \le (k_{nm}^2)_{|\min}$, where $(k_{nm}^2)_{|\min}$ is the smallest eigenvalue contributing to the right-hand side. Again, each of the two sides of (5) tends to ∞ at one of the interval boundaries and a solution $k_{(1)}$ to (5) exists in the interval.

Equivalent circuits can be associated with the setup in the vicinity of these solutions. $V = E(x_0,y_0)\ d$ is the voltage across the shorting post where d is the antenna thickness. Describing the shorting post as a δ-distributed z-directed current, the impedance Z relating voltage V and current I over the shorting post is given by $i\omega\mu_0\ dG(x_0,y_0)$. In the vicinity of k_{10} this can be written as

$$Z = \frac{i\omega L}{1-\omega^2 LC} + i\omega L_s \quad (6)$$

with

$$L = \mu_0\, d\, \frac{|\psi_{10}(x_0,y_0)|^2}{k_{10}^2} \quad (7)$$

$$C = \varepsilon \frac{1}{d|\psi_{10}(x_0,y_0)|^2} \quad (8)$$

$$L_s = \mu_0\, d \sum_{(n,m)\neq(1,0)} \frac{|\psi_{nm}(x_0,y_0)|^2}{k_{nm}^2-k^2}. \quad (9)$$

The effect of the shorting post can thus be understood as introducing a series inductance L_s to the LC-resonance circuit describing the (1,0) resonance of the unloaded patch. The associated resonance frequency is lifted to a higher value $\omega_{(1)} = \sqrt{(1/LC)+(1/L_sC)}$. In the vicinity of the zero mode, the impedance can be written as

$$Z = \frac{1}{i\omega C} + i\omega L \quad (10)$$

with

$$C = \varepsilon \frac{1}{d|\psi_{00}(x_0,y_0)|^2} \quad (11)$$

$$L = \mu_0\, d \sum_{(n,m)\neq(0,0)} \frac{|\psi_{nm}(x_0,y_0)|^2}{k_{nm}^2-k^2}. \quad (12)$$

Upon proper normalization of the ψ_{nm}, C is just the static capacitance of the patch configuration. The shorting post can therefore be understood to raise the zero eigenvalue of the unloaded patch to a value $1/\sqrt{LC}$. To summarize, the introduction of the shorting post generates a spectrum $\{k_{(i)}|i=1,2,\cdots\}$ the elements of which systematically lie above the eigenvalues of the Laplace operator including the zero eigenvalue. To identify the obtained spectrum with physically observable resonances, consider the generic case of a shorting post at (x_1,y_1) and a feed at (x_2,y_2). The input impedance of this setup is gained by relating voltage and current across the feed and the shorting post via

$$0 = Z_{11}I_1 + Z_{12}I_2 \quad (13)$$

$$V_2 = (Z_{21}I_1 + Z_{22}I_2) \quad (14)$$

$$\Rightarrow \quad V_2 = \frac{Z_{11}Z_{22}-Z_{12}Z_{21}}{Z_{11}} I_2. \quad (15)$$

This leads to the physical interpretation of the spectrum $\{k_{(i)}\}$: the input impedance, purely reactive when damping is not included, blows up when the driving frequency approaches $\omega_{(i)} = ck_{(i)}$ and the antenna displays a resonant behavior. The real case, of course, leads to damping: radiation, ohmic, and dielectric losses lead to an imaginary part of $k_{(i)}$ and the purely reactive impedance acquires an ohmic resistance.

The procedure to be followed in the case of two or more shorting posts is a straightforward extension: the electric field is now required to vanish at each of the shorting post positions. This implies demanding the determinant of the impedance matrix of the shorting-post system to vanish. Expressing the impedance matrix elements in terms of Green's function, this can again be treated as an equation for the determination of k^2.

III. Application to Rectangular and Circular MPA's

This section illustrates the above-described theory with two concrete examples, rectangular and circular MPA's. In particular, the dependence of the lowest order resonance frequencies of rectangular and circular shorting post MPA's on shorting-post position and dimension will be discussed.

Consider first a rectangular shorting-post MPA with patch side lengths a, b. For simplicity, the shorting post, located at (x_0,y_0), shall be modeled to have a square cross section Δ^2. This means that the corresponding current distribution is formulated as

$$j(x,y) = \frac{I}{\Delta} \begin{cases} \delta\left(y-y_0-\frac{\Delta}{2}\right) + \delta\left(y-y_0+\frac{\Delta}{2}\right), \\ \qquad \text{for } x \in \left[x_0-\frac{\Delta}{2}, x_0+\frac{\Delta}{2}\right] \\ \delta\left(x-x_0-\frac{\Delta}{2}\right) + \delta\left(x-x_0+\frac{\Delta}{2}\right) \\ \qquad \text{for } y \in \left[y_0-\frac{\Delta}{2}, y_0+\frac{\Delta}{2}\right] \\ 0, \quad \text{otherwise.} \end{cases} \quad (16)$$

The average voltage across the region of the shorting post can now be expressed as

$$V = i\omega\mu_0 d \int_{x_0-(\Delta/2)}^{x_0+(\Delta/2)} dx \int_{y_0-(\Delta/2)}^{y_0+(\Delta/2)} dy \int_{x_0-(\Delta/2)}^{x_0+(\Delta/2)} dx' \cdot \int_{y_0-(\Delta/2)}^{y_0+(\Delta/2)} dy'\, G(xy, x'y') j(x'y') \quad (17)$$

$$= \frac{I}{i\omega\varepsilon\dfrac{ab}{d}} + i\omega\mu I \frac{d}{ab} \sum_{(n,m)\neq(0,0)}^{\infty} \sigma_n\sigma_m \cdot \frac{\cos^2\left(\dfrac{n\pi}{a}x_0\right)\cos^2\left(\dfrac{m\pi}{b}y_0\right)}{k_{nm}^2 - k^2} g_{nm}\left(\frac{\Delta}{a}, \frac{\Delta}{b}\right) \quad (18)$$

where the explicit analytic expression for the cavity model Green's function in terms of eigenfunctions and eigenvalues has been introduced. $k_{nm}^2 := (n\pi/a)^2 + (m\pi/b)^2$ denotes the eigenfrequencies of the unloaded patch and

$$\sigma_n = \begin{cases} 1, & \text{n = 0} \\ 2, & \text{otherwise.} \end{cases} \quad (19)$$

The term

$$g_{nm}(x,y) := \frac{\sin^2\left(n\pi\dfrac{x}{2}\right)}{\left(n\pi\dfrac{x}{2}\right)^2} \frac{\sin^2\left(m\pi\dfrac{y}{2}\right)}{\left(m\pi\dfrac{y}{2}\right)^2} \quad (20)$$

introduces a suppression factor into the infinite sum. This suppression is due to the finite shorting-post extension Δ and vanishes in case of an infinitely thin shorting post. Provided k is below the lowest order eigenfrequency of the unloaded patch, the impedance relating the voltage V to the current I over the shorting post in (18) is seen to split into the static capacitance of the unloaded cavity and an inductance. The condition of zero voltage over the shorting post thus amounts to setting the impedance of a series LC circuit equal to zero

$$\omega = \frac{1}{\sqrt{L(\omega)C}}. \quad (21)$$

Clearly, the larger the inductive part will be, the smaller will be the resulting resonance frequency, i.e., the larger will be the degree of miniaturization achievable for a fixed operation frequency. The inductance

$$L = \mu\frac{d}{ab} \sum_{(n,m)\neq(0,0)}^{\infty} \sigma_n\sigma_m \cdot \frac{\cos^2\left(\dfrac{n\pi}{a}x_0\right)\cos^2\left(\dfrac{m\pi}{b}y_0\right)}{k_{nm}^2 - k^2} g_{nm}\left(\frac{\Delta}{a}, \frac{\Delta}{b}\right) \quad (22)$$

uniformly decreases with increasing value of Δ in the suppression term g_{nm}. This means that the frequency reduction will be the greater the smaller the shorting-post extension. In the limit of vanishing shorting-post extension Δ, the expression for L is logarithmically divergent. Appropriate renormalization techniques are, therefore, required to address this limiting case.

Turning to the dependence of the resonance frequency (21) on the position (x_0, y_0) of the shorting post, L is seen to attain its maximum values at the corners of the patch (where all $\cos^2$ terms in the series are equal to one).

In order to get a large degree of miniaturization for a rectangular shorting post MPA, a shorting post of small diameter thus has to be applied to one of the corners of the patch. In a next step, a feed needs to be constructed as to achieve a good $(50\ \Omega)$ match of the input impedance (15). This procedure enables a constructive decoupling of the problem of designing shorting post and feed positions and extensions for the antenna. Simulative or experimental design techniques face the problem of requiring simultaneous design of optimum relative postion of shorting post and feed for a given feed construction.

Fig. 1(a) shows the lowest resonance frequency numerically gained from (21) for a rectangular patch antenna of dimensions $a = 18.2$ mm, $b = 19.6$ mm, $d = 2$ mm on an $\varepsilon_r = 17$ substrate as a function of relative (x, y) position of the shorting post. For symmetry reasons, only a quarter of the domain is depicted. Fig. 1(b)shows a cut of this surface for different values of the feed extension Δ. The lowest order eigenvalue of the unloaded patch amounts to 1.9 GHz.

The figures confirm the discussed expectations: the lowest resonance frequency attains its minimum at the corners of the patch and decreases with decreasing feed extension. The maximum with respect to shorting-post position is reached at the center of the patch where each second contribution to the sum in (22) vanishes leading to a particularly small inductance value.

Fig. 2(a) shows the lowest order resonance frequency of a rectangular shorting-post MPA as a function of the patch surface area where one side length a is fixed to a value of 18.2 mm. The shorting-post position is fixed to a corner of the rectangle. For b smaller than a, the lowest order resonance frequency of the unloaded patch is (in the cavity model approximation) uniformly equal to 2 GHz for the chosen dielectric constant of $\varepsilon_r = 17$. However, in the loaded antenna, the lowest resonance frequency is seen to decrease with increasing patch area.

Fig. 2(b)shows the dependence of the lowest order resonance frequency as a function of the asymmetry a/b of the patch for a fixed patch surface area. Again, the shorting post is positioned at the corner of the rectangle. For comparison the corresponding variation of the unloaded patch is also given in the figure. In the loaded and the unloaded case, the resonance frequency uniformly decreases with increasing asymmetry (decreasing values of a/b). However, the largest degree of miniaturization for the loaded patch as compared to the unloaded patch of equal length ratio will be achieved at symmetric layout. Except for largely asymmetric layouts, the variation of the resonance frequency of the loaded patch is significantly weaker than for the loaded patch.

Finally, Fig. 3 gives the distribution of the electric field under the patch in the lowest order resonance as gained from a MAFIA simulation. Unlike in the situation of the lowest order resonance of the unloaded patch, the electric field is more or less constant except for the immediate vicinity of the shorting post and the cavity edges. This again clearly confirms the association of this low-frequency resonance with the zero mode of the unloaded patch.

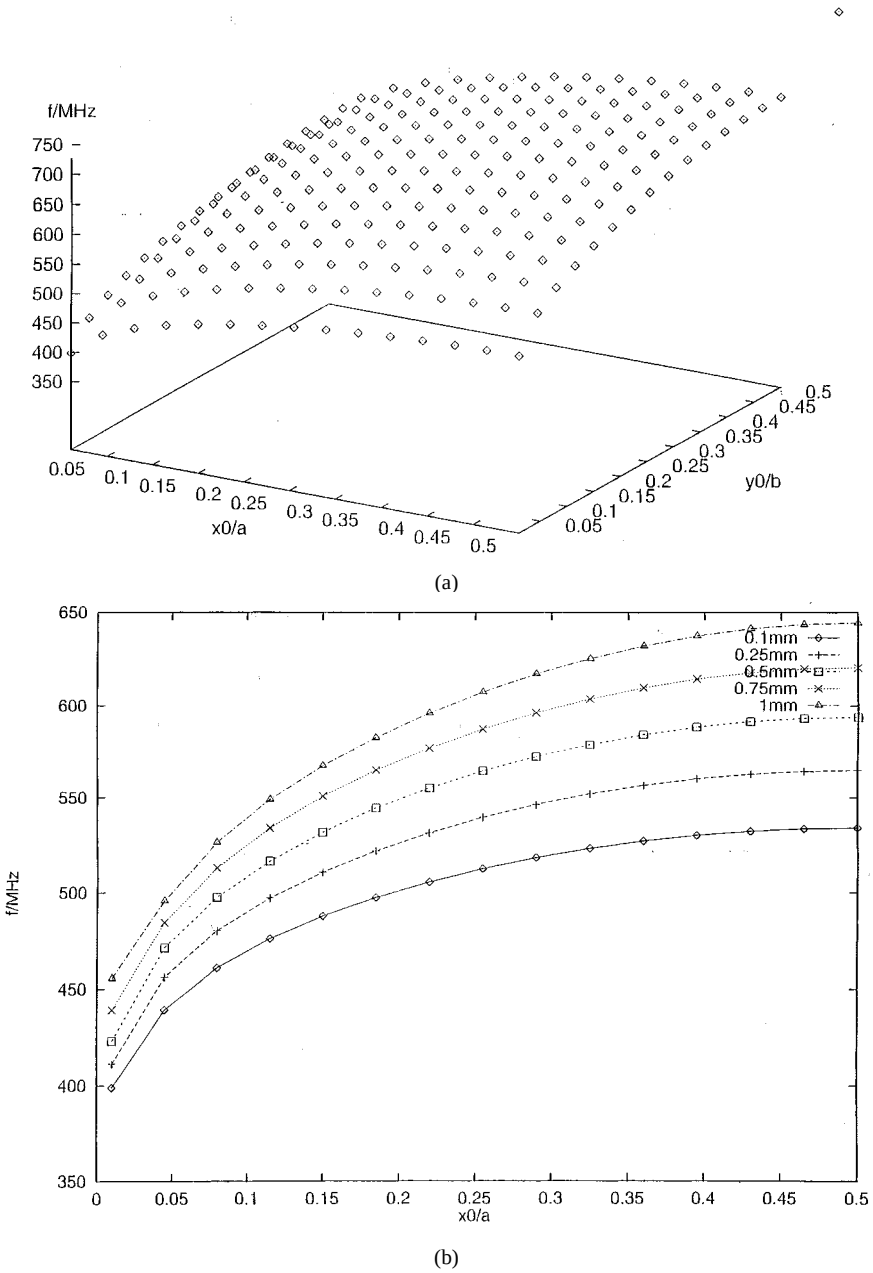

Fig. 1. (a) Lowest order resonance frequency $f_{(0)}$ of a rectangular shorting-post MPA as a function of relative shorting-post coordinates x_0/a, y_0/b. Dimensions: $a = 18.2$ mm, $b = 19.6$ mm, $t = 2$ mm, $\varepsilon = 17$, $\Delta/\sqrt{\pi} = 0.1$ mm (shorting-post extension). (b) Lowest order resonance frequency $f_{(0)}$ of rectangular shorting post MPA as a function of relative shorting-post coordinate x_0/a with fixed $y_0/b = 0.01$ and for different shorting-post extensions $\Delta/\sqrt{\pi}$ as indicated in the figure. All other parameters as in Fig. 1(a).

A determination of all relevant antenna parameters for the shorting-post MPA is straightforward once the resonance frequencies have been determined. The associated resonant modes E^i can immediately be formulated as an expansion in terms of the normalized resonant modes ψ_{nm} of the unloaded patch

$$E^i(x,y) = \sum_{n,m=0}^{\infty} a^i_{nm}\psi_{nm}(x,y) \tag{23}$$

where:

$$a^i_{nm} = \int_{x_0-(\Delta/2)}^{x_0+(\Delta/2)} dx' \int_{y_0-(\Delta/2)}^{y_0+(\Delta/2)} dy' \frac{\psi^*_{nm}(x')(y')}{k^2_{nm}-k^2_i} j(x',y') \tag{24}$$

and

$$\psi_{nm}(x,y) = \sqrt{\frac{\sigma_n\sigma_m}{ab}} \cos\left(\frac{n\pi}{a}x\right)\cos\left(\frac{m\pi}{b}y\right). \tag{25}$$

With (23) and the associated magnetic fields, the far-field radiation potentials $A(\theta,\phi)$ and with it all radiation performance parameters can simply be determined from the corresponding equivalent currents on the cavity walls. Due to the linearity of all involved equations, these vector potentials are a superposition of the well-known cavity-model expressions A^0_{nm} for the unloaded patch with mode coefficients a^i_{nm}.

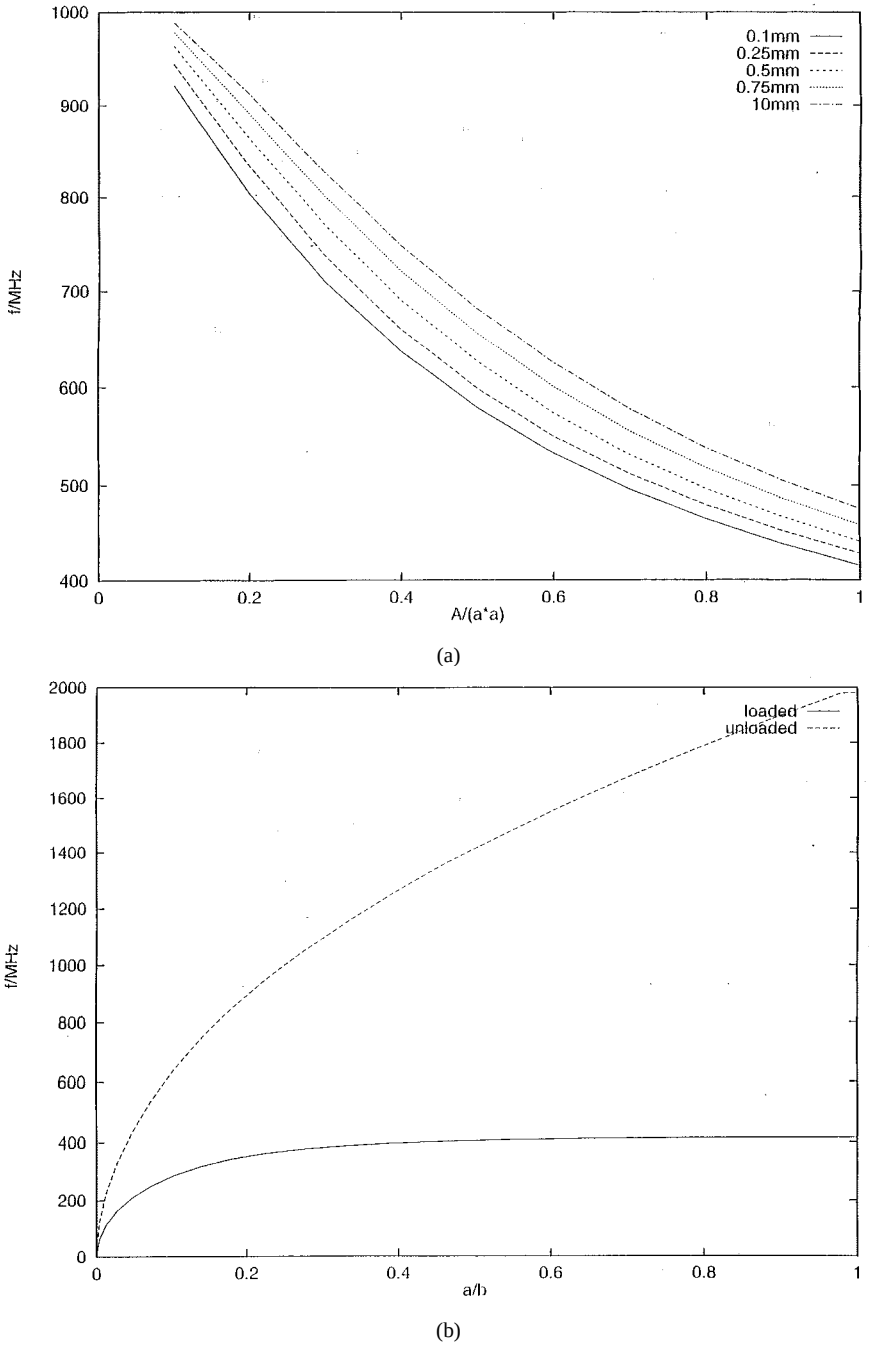

Fig. 2. (a) Lowest order resonance frequency $f_{(0)}$ of rectangular shorting post MPA as a function of relative patch surface area A/a^2. a is kept equal to 18.2 mm, $b = A/a$; different curves pertain to different shorting post extensions $\Delta/\sqrt{\pi}$ as indicated in the figure. The shorting post is positioned at a corner of the patch $(x_0, y_0) = 0.01 \times (a, b)$. All other parameters as in Fig. 1(a). (b) Lowest order resonance frequency $f_{(0)}$ of a shorting post rectangular MPA of fixed patch-surface area $A = (18.2 \text{ mm})^2$ as a function of the asymmetry b/a. The shorting post is positioned at a corner of the patch $(x_0, y_0) = 0.01 \times (a, b)$; $\Delta/\sqrt{\pi} = 0.1$ mm. All other parameters as in Fig. 1(a). For reference, the corresponding values for an unloaded patch are also given.

Consider, as a second example, a circular shorting post MPA of patch radius r. The Green's function for the unloaded configuration is given by

$$G(r\phi, r'\phi') = \frac{1}{i\omega\varepsilon\pi a^2} + i\omega\mu \sum_{n=0}^{\infty}\sum_{m=1}^{\infty} f\sigma_n J_n(k_{nm}r) J_n(k_{nm}r') \cdot \frac{\cos(n(\phi - \phi'))}{\pi\left(a^2 - \frac{n^2}{k_{nm}^2}\right)(k_{nm}^2 - k^2) J_n^2(k_{nm}a)} \quad (26)$$

where the resonance frequencies k_{nm} are determined by

$$\partial_r J_{nm}(k_{nm}r)_{|r=a} = 0. \quad (27)$$

For the zeroth-order Bessel function, the first root is taken to be the nonzero root.

To calculate the average voltage across the shorting post, the latter is modeled as a cylindrical current distribution so that the

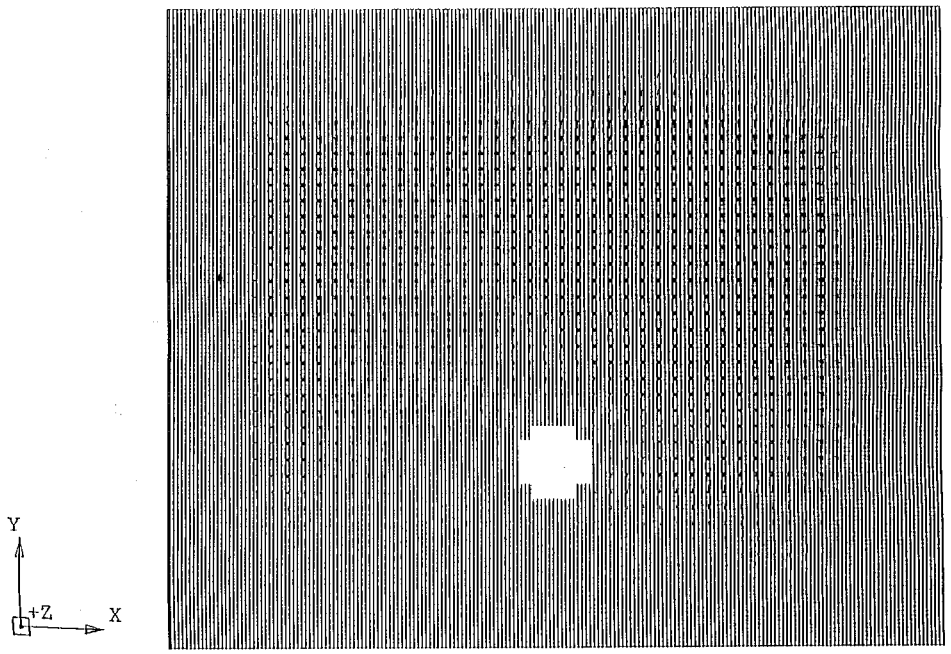

Fig. 3. Distribution of electrical field in a generic rectangular shorting-post MPA as gained from a MAFIA-package simulation. The dot size corresponds to the field strength.

Green's function will be integrated over the (r, ϕ) domain

$$\left(r_0 + \frac{\Delta}{2}\cos\alpha, \phi_0 + \frac{\Delta}{2r_0}\sin\alpha\right) \qquad \alpha \in [0, 2\pi] \tag{28}$$

in both of its variable pairs. (r_0, ϕ_0) denotes the feed-center position and $\Delta \ll a$ its diameter. This procedure for accounting for a small circular current distribution in a circular patch is, e.g., described in [7]. Finally, the impedance to be set equal to zero for obtaining the resonance frequencies of the loaded patch is given by

$$Z(\omega) = \frac{d}{i\omega\varepsilon\pi a^2} + i\omega\mu d \sum_{n=0}^{\infty}\sum_{m=1}^{\infty} \sigma_n \cdot \frac{J_n^2(k_{nm}r_0)}{\pi\left(a^2 - \frac{n^2}{k_{nm}^2}\right)(k_{nm}^2 - k^2)J_n^2(k_{nm}a)} g_n(\Delta) \tag{29}$$

where the suppression term due to the finite-feed extension is given by

$$g_n(\Delta) = J_0^2\left(n\frac{\Delta}{2r_0}\right). \tag{30}$$

Fig. 4 shows the variation of the lowest resonance frequency of a loaded circular MPA as a function of the relative radial shorting-post position r_0/a for various shorting post radii. The patch is dimensioned as to give a lowest order resonance at 2 GHz in the unloaded case. This means that the patch has the same area as the rectangular patch considered in Fig. 1. As in the case of the rectangular MPA, larger shorting post radii lead to stronger supression of the inductive part of the shorting-post impedance and, therefore, to higher resonance frequencies. The lowest values for the resonance frequency are obtained when positioning the shorting post at the edge of the patch. In general, the resonance frequencies obtainable from a loaded circular patch are larger than those of a rectangular patch of equal cross section. Therefore, a stronger miniaturization is possible for a loaded rectangular MPA. It is also seen that the sensitivity of the resonance frequency against variations of the shorting-post position of the circular MPA is stronger than in the rectangular case.

As in the case of the rectangular MPA, calculation of the resonance modes and radiation properties is a straightforward task.

To conclude the discussion, an indication of the numerical accuracy of the model shall be given. Table I compares the lowest order resonance frequency for different shape shorting-post MPA's to corresponding measured and/or simulated minimum return loss positions. A coaxial feed was employed in the simulations and measurements. The HP HFSS package was used to carry out the numerical simulations.

Frequency eigenvalues and minimum $|S_{11}|$ positions do, in general, not exactly coincide; systematically higher values for the latter must be expected. Taking this into account, the cursory comparison indicates that even the quantitative predictive power of the presented fully anlaytic model is remarkable.

IV. Conclusions

A Green's function-based theory for analytically deriving the eigenfrequency spectrum of shorting-post MPA's has been developed. This theory allows for a comprehensive calculation of all relevant performance parameters of such antennas. The central role of the zero mode of the unloaded MPA for reducing the

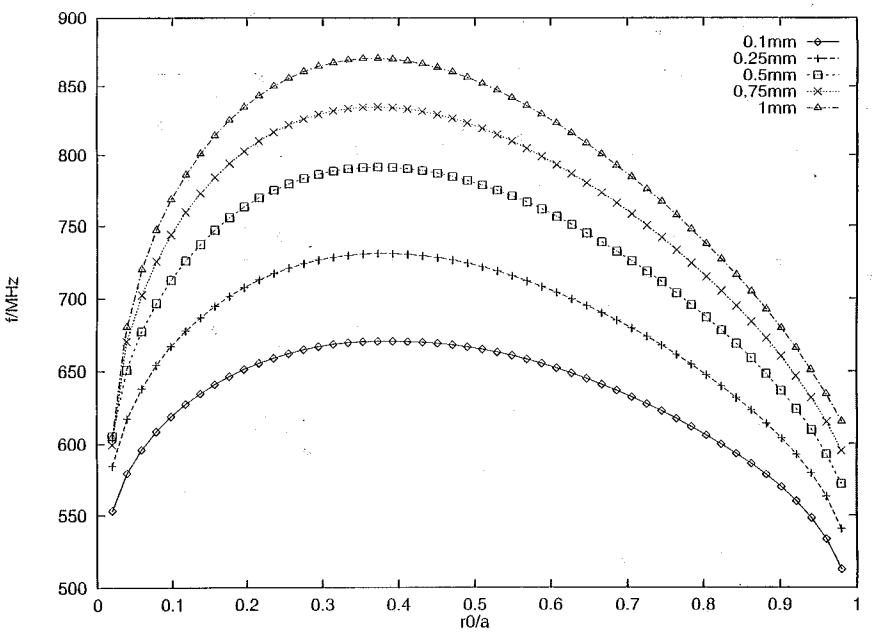

Fig. 4. Lowest order resonance frequency $f_{(0)}$ of a circular shorting-post MPA as a function of relative shorting post position r_0/a for different shorting-post diameters Δ as indicated in the figure. Dimensions: $a = 10.7$ mm, $t = 2$ mm, $\varepsilon = 17$.

TABLE I
QUANTITATIVE COMPARISON OF LOWEST ORDER RESONANCE FREQUENCIES AS PREDICTED BY THE PRESENTED THEORY TO SIMULATED (s) AND/OR MEASURED (m) MINIMUM $|S_{11}|$ POSITION FOR VARIOUS SHORTING-POST MPA CONFIGURATIONS

patch shape	circle	annular ring	rectangle
lateral dimensions	$r = 9.19$	$r_1 = 9.2\,mm$ $r_2 = 18.4\,mm$	$a = 13\,mm$ $b = 19.5\,mm$
substrate thickness	$1.524\,mm$	$3.18\,mm$	$1.4\,mm$
ε_r	4.81	17	17
shorting post position	$r_0 = 7\,mm$	$r_0 = 10.7\,mm$	$x_0 = 1.1\,mm$, $y_0 = 0.5b$
shorting post radius	$0.3\,mm$	$0.25\,mm$	$1\,mm$
f_{res}/MHz, theory	1484	362	904
f/MHz (min. $\|S_{11}\|$)	1540[1] (s) 1534[2] (m)	380 (m)	957 (s)
offset	3.6% 3.3%	4.7%	5.5%

operation frequency of a shorting-post MPA has been revealed and thoroughly discussed.

The practical application of this scheme has been demonstrated on the examples of rectangular and circular shorting post MPA's.

ACKNOWLEDGMENT

The author would like to thank K. Dietz and her colleagues, particularly I. Ghosh, for stimulating discussions on the subject.

REFERENCES

[1] Y. P. Zhang *et al.*, "A dielectric loaded miniature antenna for microcellular and personal communication," in *Proc. IEEE AP-Symp.*, Newport Beach, CA, June 1995, pp. 1152–1155.
[2] Y. Hwang *et al.*, "Planar inverted-F antenna loaded with high permittivity material," *Electron. Lett.*, vol. 31, pp. 1710–1712, Sept. 1995.
[3] T. K. Lo *et al.*, "Miniature aperture-coupled microstrip antenna of very high directivity," *Electron. Lett.*, vol. 33, pp. 9–10, 1997.
[4] N. G. Alexopoulos and D. R. Jackson, "Fundamental superstrate (cover) effects on printed circuit antennas," *IEEE Trans. Antennas Propagat.*, vol. AP-32, pp. 807–816, Aug. 1984.
[5] R. Waterhouse, "Small microstrip patch antenna," *Electron. Lett.*, vol. 31, pp. 604–605, 1995.
[6] S. Dey and R. Mittra, "Compact microstrip patch antenna," *Microwave Opt. Technol. Lett.*, vol. 13, pp. 12–14, Sept. 1996.
[7] K. L. Wong and S. C. Pan, "Compact triangular microstrip antenna," *Electron. Lett.*, vol. 33, pp. 433–434, 1997.
[8] D. M. Kokotoff *et al.*, "An annular ring coupled to a shorted patch," *IEEE Trans. Antennas Propagat.*, vol. 45, pp. 913–914, May 1997.
[9] D. Schaubert *et al.*, "Microstrip antennas with frequency agility and polarization diversity," *IEEE Trans. Antennas Propagat.*, vol. AP-29, pp. 118–123, Jan. 1981.
[10] W. F. Richards and Y. T. Lo, "Theoretical and experimental investigation of a microstrip radiator with multiple lumped linear loads," *Electromagn.*, vol. 3, pp. 371–385, 1983.
[11] W. F. Richards, S. E. Davidson, and S. A. Long, "Dual-band reactively loaded microstrip antenna," *IEEE Trans. Antennas Propagat.*, vol. AP-33, pp. 556–561, May 1985.
[12] S. Tokumaru and S. Fukui, "Microstrip antennas having posts for circular polarization," *Electron. Commun. Japan*, vol. 67-B, pp. 75–85, 1984.

Rebekka Porath was born in Düsseldorf, Germany. She received the Diploma degree in physics and the Ph.D. degree in theoretical physics, both from the Rheinische-Friedrich-Wilhelms-University Bonn, Germany, in 1991 and 1994, respectively.

Since 1995, she has been with the Philips Research Laboratories in Aachen, Germany, where she is currently project leader for high-frequency components. Her research interests include application, concepts and design of HF components for mobile telecommunication, and module integration techniques.